Analysis of Exoskeleton based on a Light Underactuated Hand

Denan Liang [1, †, *], Xin Jiang [2, †], Wenhan Zhang [3]

[1] Dublin School of International Transport, Chang 'an University, Xi'an, China

[2] Institute of Technology, Wenzhou Kean University, Wenzhou, China

[3] School of International Education Yantai Institute of Technology, Yantai, China

[*] Corresponding author Email: 2021905146@chd.edu.cn

[†]These authors contributed equally

Abstract. The number of stroke patients is increasing year by year, and the demand for rehabilitation medical equipment is also increasing. The number of stroke patients is increasing year by year, and the demand for rehabilitation medical machinery is also increasing. The hand exoskeleton machinery plays an indispensable role in the rehabilitation process. In the treatment, the hand exoskeleton machinery equipment needs to be convenient, easy to air, lightweight, and meet the needs of human hands. Robhand meets these requirements in design, but the rotation range of MCP joint and PIP joint of index finger can't meet the needs of treatment. In this paper, the vector equations of the two loops are obtained through the kinematic modeling of Robhand and the kinematic analysis, and then the numerical solution is obtained by the numerical solution of MATLAB, that is, the Rotation angle of the mechanism φ Rotation angle with MCP joint αand PIP joint β.

Keywords: Hand Exoskeleton; Motion Range; Kinematic Analysis; Numerical Solution.

1. Introduction

With the aging of the world population, stroke has become one of the three fatal diseases of human beings [1], which has the characteristics of high incidence rate, high mortality in order to high disability rate [2]. It is estimated that stroke is the cause of death of 4.5 million people every year. In addition, the incidence rate of men over 45 years old and elderly women is particularly high. In recent years, the total incidence rate has reached five cases per 1000 people, and stroke has become the main cause of middle-aged disability [3]. The main method of finger motor rehabilitation after stroke is to improve the hand motor function of patients by implementing rehabilitation training of motor function [4]. But at present, there are many patients and few rehabilitation doctors around the world. To solve this problem, the research and development of hand exoskeleton robots have been promoted. Exoskeleton robot technology is a comprehensive technology of provides a wearable mechanical mechanism for operators, which integrates sensing, control, information, fusion and mobile computing. Underactuated robots are a class of robots that have fewer independent control inputs than the system's degrees of freedom, and for underactuated machines, a joint or joints that do not contain a drive, i.e., the joints are passive, also known as free. Robots that are underactuated offer various benefits, including being lightweight, inexpensive, and energy efficient. Underactuated robots are considerably different from conventional robots in terms of control since they require less input to generate motion in more bit-shaped regions [5]. In the following circumstances, robots typically exhibit underactuated characteristics: 1) In bionic robots, underactuated joints are utilized to achieve efficient and graceful mobility that is inspired by human movement. 2) In space robots, microgravity settings, or some especially small systems, underactuated joints can significantly reduce weight and cost. 3) The design of a deliberate reduction in the number of drives to maximize system dexterity. 4) The system itself has some motion limits and becomes an underactuated system, such as a mobile robot. Underactuated hand robots belong to the first case [6]. The underactuated hand robot is a new type of multi-purpose hand robot. This type of hand robot has the peculiarity that there are fewer drive elements than there are degrees of freedom in the finger joints. The hand robot contains a minimal number of drive elements (motors) and only one drive source per finger, which simplifies

the complexity of the structure and operation and offers the benefits of easy control and a large grasping range. Strong envelope gripping via underactuated and precision grasping via end-joint pinching is also achievable. The underactuated connecting rod chute exoskeleton designed by Nanjing University of technology can reduce the weight of the structure by reducing the drive on the premise of supporting multi-degree of a freedom movement, thereby achieving lightness and improving patient comfort when wearing it [7]. Shanghai Jiao Tong University has designed a lightweight hand exoskeleton based on linear motor drive, which has an overall weight of 402g and meets the patient's need for small size and portability. Currently, finger exoskeleton robots are trending towards small size, lightweight, and portability in terms of structure; and towards a combination of multiple movements states in terms of function [8]. However, because of the unique features of the underactuated mechanism, the underactuated hand robot will experience contact point disengagement during the process of clutching an envelope, which will compromise the stability of the underactuated hand claw gripping [9]. The underactuated robot's dynamics model resembles the fully driven robots in shape and can include one or more passive joints. Despite being conceptually identical to the fully driven robot in model form, the underactuated robot's equations of motion have incomplete restrictions, which causes the control strategies for the two systems to differ. The underactuated hand robot must have correct control, so it has to have its dynamics modeled and its dynamical traits examined [10]. Robhand meets the above requirements, which is an underactuated design. Victor Moreno San Juan et al. Carried out structural characteristics, mechanical design ,and kinematic model of robhand and evaluated it [11]. However, the rotation angle of the MCP joint and PIP joint cannot reach the maximum rotation angle of the human index finger, that is, it cannot fully meet the needs of human hands. In this paper, the kinematic equations are analyzed and the rotation angle of the mechanism is obtained by using MATLAB φ Rotation angle with MCP joint α.

2. Method

2.1 Kinematic Model

The Robhand planar linkage mechanism is shown in Fig.1.a, and the line parameters and angle parameters are shown in Fig. 1b and c.

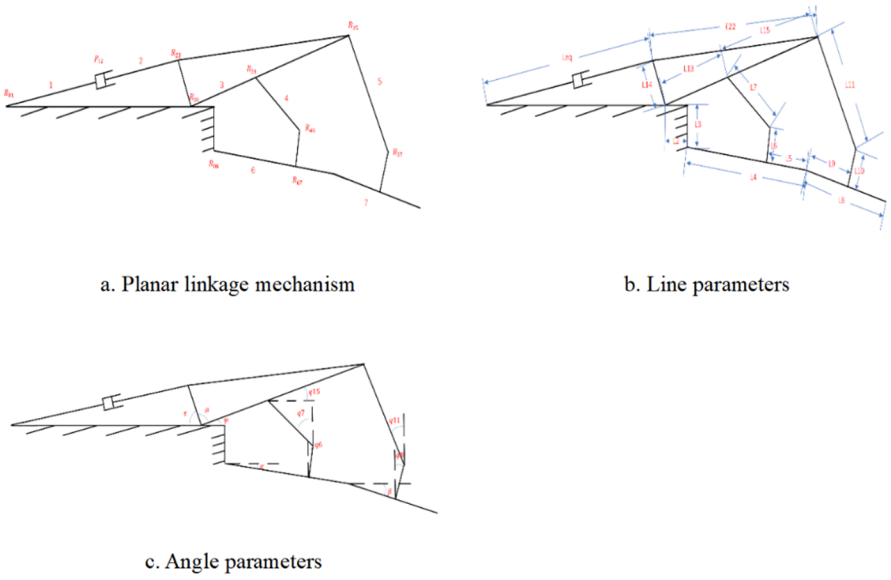

a. Planar linkage mechanism

b. Line parameters

c. Angle parameters

Fig 1. Repression of the planer bar-linkage mechanism of one finger

2.1.1 Kinematic Equation for Loop 1

The mechanism is composed of two mechanical closed loops. As shown in Fig.2.a and b, the parameters in each closed loop are defined by vector equations.

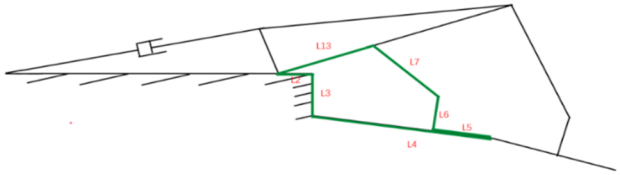

a. Loop 1

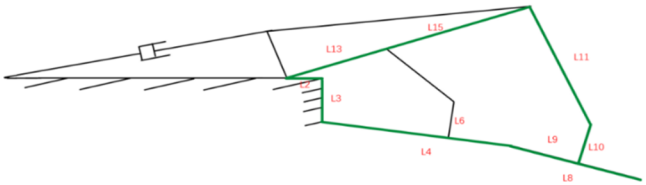

b. Loop 2

Fig 2. Two mechanical closed loops

Loop1:

The closed-loop vector equation can be obtained from Euler identity:

$$\overrightarrow{l_2}+\overrightarrow{l_3}+\overrightarrow{l_4}-\overrightarrow{l_5}+\overrightarrow{l_6}+\overrightarrow{l_7}+\overrightarrow{l_{13}}=0 \tag{1}$$

Decompose it on the x-axis and y-axis to obtain:

$$\begin{cases} \overrightarrow{l_2}+(\overrightarrow{l_4}-\overrightarrow{l_5})\cos\alpha+\overrightarrow{l_6}\sin q_6+\overrightarrow{l_7}\sin q_7-\overrightarrow{l_{13}}\cos\varphi=0 \text{ (a)} \\ -\overrightarrow{l_3}+(\overrightarrow{l_4}-\overrightarrow{l_5})\sin\alpha+\overrightarrow{l_6}\cos q_6+\overrightarrow{l_7}\cos q_7-\overrightarrow{l_{13}}\sin\varphi=0 \text{ (b)} \end{cases} \tag{2}$$

Fig. 1. c. shows that $\alpha = q_6$.Variables $\{\varphi,\ \alpha,\ q_7\}$ are taken, with φ being the independent variable, and $\{\alpha,\ q_7\}$ dependent variables. Through mathematical operation and PYTHON, the relationship of φ and α can be obtained.

2.1.2 Derivation and Calculation of Kinematic Equation for Loop 1

Move the term obtaining q_7 to the right of equation:

$$\begin{cases} \overrightarrow{l_2}+(\overrightarrow{l_4}-\overrightarrow{l_5})\cos\alpha+\overrightarrow{l_6}\sin q_6-\overrightarrow{l_{13}}\cos\varphi=-\overrightarrow{l_7}\sin q_7 \text{ (a)} \\ -\overrightarrow{l_3}+(\overrightarrow{l_4}-\overrightarrow{l_5})\sin\alpha+\overrightarrow{l_6}\cos q_6-\overrightarrow{l_{13}}\sin\varphi=-\overrightarrow{l_7}\cos q_7 \text{ (b)} \end{cases} \tag{3}$$

Squaring both sides of equation:

$$\begin{cases} [\overrightarrow{l_2}+(\overrightarrow{l_4}-\overrightarrow{l_5})\cos\alpha+\overrightarrow{l_6}\sin q_6-\overrightarrow{l_{13}}\cos\varphi]^2=(-\overrightarrow{l_7}\sin q_7)^2 \text{ (a)} \\ [-\overrightarrow{l_3}+(\overrightarrow{l_4}-\overrightarrow{l_5})\sin\alpha+\overrightarrow{l_6}\cos q_6-\overrightarrow{l_{13}}\sin\varphi]^2=(-\overrightarrow{l_7}\cos q_7)^2 \text{ (b)} \end{cases} \tag{4}$$

Sum Eqs.(4)(a) and (4)(b). Obtaining the equation of φ and α.

$$\begin{aligned} &[\overrightarrow{l_2}+(\overrightarrow{l_4}-\overrightarrow{l_5})\cos\alpha+\overrightarrow{l_6}\sin q_6-\overrightarrow{l_{13}}\cos\varphi]^2+[-\overrightarrow{l_3}+(\overrightarrow{l_4}-\overrightarrow{l_5})\sin\alpha+\overrightarrow{l_6}\cos q_6-\overrightarrow{l_{13}}\sin\varphi]^2 \\ &=(-\overrightarrow{l_7}\cos q_7)^2+(-\overrightarrow{l_7}\sin q_7)^2 \end{aligned} \tag{5}$$

Take apart the square term:

$$
\begin{aligned}
&l_2^{\,2}+[(l_4-l_5)\cos\alpha]^2+(l_6\sin\alpha)^2+(-l_{13}\cos\varphi)^2+2l_2(l_4-l_5)\cos\alpha\\
&+2l_2l_6\sin\alpha-2l_2l_{13}\cos\varphi+2l_6(l_4-l_5)\sin\alpha\cos\alpha-2l_{13}(l_4-l_5)\cos\alpha\cos\varphi\\
&-2l_6l_{13}\sin\alpha\cos\varphi+(-l_3)^2+[(l_4-l_5)\sin\alpha]^2+(l_6\cos\alpha)^2+(-l_{13}\sin\varphi)^2\\
&-2l_3(l_4-l_5)\sin\alpha-2l_3l_6\cos\alpha+2l_3l_{13}\sin\varphi-2l_{13}(l_4-l_5)\sin\alpha\sin\varphi\\
&-2l_6l_{13}\cos\alpha\sin\varphi+2l_6(l_4-l_5)\sin\alpha\cos\alpha=l_7^{\,2}
\end{aligned}
\tag{6}
$$

By formula $cosA^2 + sinA^2 = 1$ to simplify:

$$
\begin{aligned}
&l_2^{\,2}+(l_4-l_5)^2+l_6^{\,2}+l_{13}^{\,2}+2(l_4-l_5)(l_2\cos\alpha-l_3\sin\alpha)+2l_6(l_2\sin\alpha-l_3\cos\alpha)\\
&+2l_{13}(l_3\sin\varphi-l_2\cos\varphi)-2l_{13}(l_4-l_5)(\cos\alpha\cos\varphi+\sin\alpha\sin\varphi)\\
&-2l_6l_{13}(\sin\alpha\cos\varphi+\cos\alpha\sin\varphi)+4l_6(l_4-l_5)\sin\alpha\cos\alpha=l_7^{\,2}
\end{aligned}
\tag{7}
$$

Move the term without variables to the right of the equal sign and simplify using the sum of two angles formula:

$$
\begin{aligned}
&[2l_2(l_4-l_5)-2l_6l_3]\cos\alpha+[2l_6l_2-2l_3(l_4-l_5)]\sin\alpha-2l_{13}(l_4-l_5)\cos(\alpha-\varphi)\\
&+2l_{13}l_3\sin\varphi-2l_{13}l_2\cos\varphi-2l_6l_{13}\sin(\alpha+\varphi)+2l_6(l_4-l_5)\sin2\alpha\\
&=l_7^{\,2}-l_2^{\,2}-(l_4-l_5)^2-l_6^{\,2}-l_{13}^{\,2}
\end{aligned}
\tag{8}
$$

To calculate Eqs. (8), It is necessary to provide the values of geometric parameters representing human fingers and the lengths of each rod. The parameters of fingers are based on data from [9]. And all the rod lengths are obtained through proportional operation.

Unit: mm

$l_2=8.486,\ l_3=28.28,\ l_4=42.43,\ l_5=10.6,\ l_6=14.14,\ l_7=28.28,\ l_8=28.28$

$l_9=9.54,\ l_{10}=14.14,\ l_{11}=45.25,\ l_{13}=28.28$

Bring the parameters into Eqs.(8)

$$
\begin{aligned}
&-259.54\cos\alpha-1560.32\sin\alpha+1599.52\sin\varphi-479.97\cos\varphi\\
&-1800.3\cos(\alpha-\varphi)+900.15\sin2\alpha-799.76\sin(\alpha+\varphi)=-2012.85
\end{aligned}
\tag{9}
$$

2.1.3 Kinematic Equation for Loop 2

Loop 2:

The closed-loop vector equation can be obtained from Euler identity:

$$
\vec{l}_2+\vec{l}_3+\vec{l}_4+\vec{l}_9+\vec{l}_{10}+\vec{l}_{11}+\vec{l}_{15}+\vec{l}_{13}=0 \tag{10}
$$

Decompose it on the x-axis and y-axis to obtain:

$$
\begin{cases}
\vec{l}_2+\vec{l}_4\cos\alpha+\vec{l}_9\cos\beta-\vec{l}_{10}\sin q_8+\vec{l}_{11}\sin q_{11}-\vec{l}_{15}\cos q_{15}-\vec{l}_{13}\cos\varphi=0 \text{ (a)}\\
-\vec{l}_3+\vec{l}_4\sin\alpha+\vec{l}_9\sin\beta+\vec{l}_{10}\cos q_8+\vec{l}_{11}\cos q_{11}-\vec{l}_{15}\sin q_{15}-\vec{l}_{13}\sin\varphi=0 \text{ (b)}
\end{cases}
\tag{11}
$$

Fig.1. c. shows that $\beta = q_8$and $\varphi = q_8$.Variables $\{\varphi,\ \alpha,\ q_{11},\ \beta\}$ are taken, with φ being the independent variable, and $\{\alpha,\ q_7,\ \beta\}$ dependent variables. Through mathematical operation and PYTHON, the relationship of φ and β can be obtained.

2.1.4 Derivation and Calculation of Kinematic Equation for Loop 2

Move the term obtaining q_{11} to the right of equation:

$$
\begin{cases}
\vec{l}_2+\vec{l}_4\cos\alpha+\vec{l}_9\cos\beta-\vec{l}_{10}\sin\beta-(\vec{l}_{15}+\vec{l}_{13})\cos\varphi=-\vec{l}_{11}\sin q_{11} \text{ (a)}\\
-\vec{l}_3+\vec{l}_4\sin\alpha+\vec{l}_9\sin\beta+\vec{l}_{10}\cos q_\beta-(\vec{l}_{15}+\vec{l}_{13})\sin\varphi=-\vec{l}_{11}\cos q_{11} \text{ (b)}
\end{cases}
\tag{12}
$$

Squaring both sides of equation:

$$
\begin{cases}
[\vec{l}_2+\vec{l}_4\cos\alpha+\vec{l}_9\cos\beta-\vec{l}_{10}\sin\beta-(\vec{l}_{15}+\vec{l}_{13})\cos\varphi]^2=(-\vec{l}_{11}\sin q_{11})^2 \text{ (a)}\\
[-\vec{l}_3+\vec{l}_4\sin\alpha+\vec{l}_9\sin\beta+\vec{l}_{10}\cos q_\beta-(\vec{l}_{15}+\vec{l}_{13})\sin\varphi]^2=(-\vec{l}_{11}\cos q_{11})^2 \text{ (b)}
\end{cases}
\tag{13}
$$

Sum Eqs. (13)(a) and (13)(b). Obtaining the equation of φ, α, β.

$$\begin{aligned}&[\overrightarrow{l_2}+\overrightarrow{l_4}\cos\alpha+\overrightarrow{l_9}\cos\beta-\overrightarrow{l_{10}}\sin\beta-(\overrightarrow{l_{15}}+\overrightarrow{l_{13}})\cos\varphi]^2+[-\overrightarrow{l_3}+\overrightarrow{l_4}\sin\alpha\\&+\overrightarrow{l_9}\sin\beta+\overrightarrow{l_{10}}\cos q_\beta-(\overrightarrow{l_{15}}+\overrightarrow{l_{13}})\sin\varphi]^2=(-\overrightarrow{l_{11}}\cos q_{11})^2+(-\overrightarrow{l_{11}}\sin q_{11})^2\end{aligned}\tag{14}$$

Take apart the square term:

$$\begin{aligned}&l_2^2+(l_4\cos\alpha)^2+(l_9\cos\beta)^2+(l_{10}\sin\beta)^2+[(l_{15}+l_{13})\cos\varphi]^2+2l_2l_4\cos\alpha\\&+2l_2l_9\cos\beta+2l_4l_9\cos\alpha\cos\beta-2l_2l_{10}\sin\beta-2l_4l_{10}\sin\beta\cos\alpha-2l_9l_{10}\sin\beta\cos\beta\\&-2l_2(l_{15}+l_{13})\cos\varphi-2l_4(l_{15}+l_{13})\cos\varphi\cos\alpha-2l_9(l_{15}+l_{13})\cos\varphi\cos\beta\\&-2l_{10}(l_{15}+l_{13})\cos\varphi\sin\beta+l_3^2+(l_4\sin\alpha)^2+(l_9\sin\beta)^2+(l_{10}\cos\beta)^2\\&+[(l_{15}+l_{13})\sin\varphi]^2-2l_3l_4\sin\alpha-2l_3l_9\sin\beta-2l_4l_9\sin\alpha\sin\beta-2l_3l_{10}\cos\beta\\&+2l_4l_{10}\sin\alpha\cos\beta+2l_9l_{10}\sin\beta\cos\beta+2l_3(l_{15}+l_{13})\sin\varphi-2l_4(l_{15}+l_{13})\sin\varphi\sin\alpha\\&-2l_9(l_{15}+l_{13})\sin\varphi\sin\beta-2l_{10}(l_{15}+l_{13})\sin\varphi\cos\beta=l_{11}^2\end{aligned}\tag{15}$$

By formula $cosA^2+sinA^2=1$ to simplify and move the term without variables to the right of the equal sign:

$$\begin{aligned}&2l_2l_4\cos\alpha-2l_3l_4\sin\alpha-(2l_2l_{10}+2l_3l_9)\sin\beta+(2l_2l_9-2l_3l_{10})\cos\beta\\&+2l_3(l_{15}+l_{13})\sin\varphi-2l_2(l_{15}+l_{13})\cos\varphi+2l_4l_9(\cos\alpha\cos\beta-\sin\alpha\sin\beta)\\&+2l_4l_{10}(\sin\alpha\cos\beta-\sin\beta\cos\alpha)-2l_{10}(l_{15}+l_{13})(\cos\varphi\sin\beta+\sin\varphi\cos\beta)\\&-2l_4(l_{15}+l_{13})(\cos\varphi\cos\alpha+\sin\varphi\sin\alpha)-2l_9(l_{15}+l_{13})(\cos\varphi\cos\beta+\sin\varphi\sin\beta)\\&=l_{11}{}^2-l_2{}^2-l_3{}^2-l_4{}^2-l_9{}^2-l_{10}{}^2-(l_{15}+l_{13})^2\end{aligned}\tag{16}$$

Simplify using the sum of two angles formula:

$$\begin{aligned}&2l_2l_4\cos\alpha-2l_3l_4\sin\alpha-(2l_2l_{10}+2l_3l_9)\sin\beta+(2l_2l_9-2l_3l_{10})\cos\beta\\&+2l_3(l_{15}+l_{13})\sin\varphi-2l_2(l_{15}+l_{13})\cos\varphi+2l_4l_9\cos(\alpha+\beta)+2l_4l_{10}\sin(\alpha-\beta)\\&-2l_{10}(l_{15}+l_{13})\sin(\varphi+\beta)-2l_4(l_{15}+l_{13})\cos(\varphi-\alpha)-2l_9(l_{15}+l_{13})\cos(\varphi-\beta)\\&=l_{11}{}^2-l_2{}^2-l_3{}^2-l_4{}^2-l_9{}^2-l_{10}{}^2-(l_{15}+l_{13})^2\end{aligned}\tag{17}$$

Bring the parameters into Eqs. (17)

$$\begin{aligned}&720.12\cos\alpha-2399.84\sin\alpha-779.57\sin\beta+637.85\cos\beta+4320.05\sin\varphi\\&-1296.32\cos\varphi+809.56\cos(\alpha+\beta)+1199.92\sin(\alpha-\beta)-2160\sin(\varphi+\beta)\\&-6481.6\cos(\varphi-\alpha)-1457.33\cos(\varphi-\beta)=-6749.36\end{aligned}\tag{18}$$

3. Results

Taking Eqs. (9) as an indeterminate equation, and let φ range from -60 ° to 30 ° with an interval of 10 °. The numerical solution can be obtained by numerical calculation with PYTHON on the Table 1.

Table 1. The numerical solution of α and φ

Numerical solution φ	Angle	Numerical solution α	Angle
-0.17453293	-10°	-0.59522071	-34°
-0.34906585	-20°	-0.72946149	-42°
-0.52359878	-30°	-0.85685993	-49°
-0.69813170	-40°	-0.97931128	-56°
-0.87266463	-50°	-1.09698995	-63°
-1.04719755	-60°	-1.2081896	-69°
0.17453293	10°	-0.28705328	-16°
0.34906585	20°	-0.09352945	-5.4°
0.52359878	30°	0.1484146	-8.5°

Taking Eqs. (18) as an indeterminate equation, and take the values of α and β in Table 1 as constant values. The numerical solution can be obtained by numerical calculation with PYTHON on the table 2.

Table 2. The numerical solution of β and φ

Numerical solution φ	Angle	Numerical solution β	Angle
-0.17453293	-10°	-0.28105529	-16°
-0.34906585	-20°	-0.44592072	-26°
-0.52359878	-30°	-0.67410077	-39°
-0.69813170	-40°	-1.05691726	-61°
0.17453293	10°	-0.05363144	-3°
0.34906585	20°	0.00921627	0.5°
0.52359878	30°	0.02392125	2°

Make the data into a visual graph, when α is positive, the finger flexes and stretches; when α negative, finger bends.

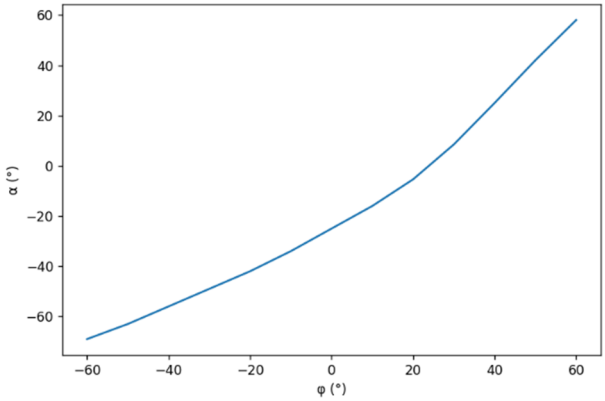

Fig 3. The relationship between φ and α

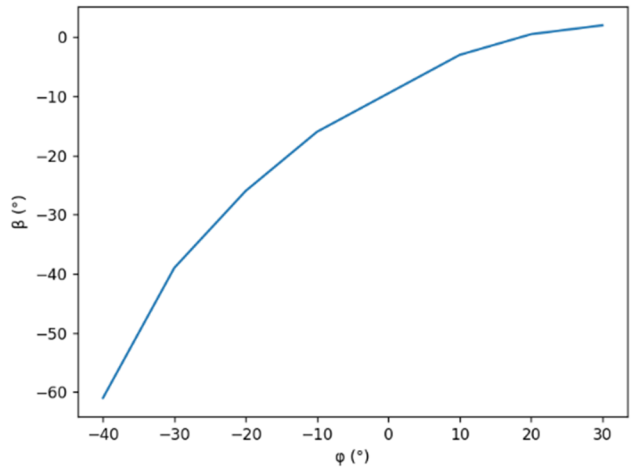

Fig 4. The relationship between φ and β

The finger flexes and stretches when α and β is positive; finger bends when α and β negative.

4. Conclusion

This research is based on a light underactuated hand exoskeleton robot that has been proposed. First, according to the prototype, the planer linkage diagram is drawn and the angle parameters and the line parameters are given. Then, the Euler equation is obtained according to the mechanical closed

loop. Obtaining the ternary nonlinear formula, obtaining a 2-variable first-order equation. Bringing all parameters into the equation and using Python to find the numerical solution. Final, obtaining the relationship between φ and α, β. Though mathematical analysis, giving the theoretical support of the mechanism.

References

[1] Liu Dongtao, Hu Wenli. Analysis of factors influencing stroke prognosis. Stroke and Neurological Disorders, 2008.

[2] Han Long. Research progress in rehabilitation training for movement disorders caused by stroke[J]. 2021.

[3] Wolfe C D A. The impact of stroke. British medical bulletin, 2000, 56(2): 275-286.

[4] Liu Lijuan. The effect of postoperative rehabilitation function exercise on the rehabilitation of stroke patients [J]. Massage and Rehabilitation Medicine, 2014.

[5] Chen Wei, Yu Yueqing, Zhang Xuping. A Survey of the Control Ability of Underactuated Robots. Industrial Instruments and Automation Devices, 2006.

[6] Chen Wei, Yu Yueqing, Zhang Xuping. A Survey on the Underactuated Robots. Machine Design and Research, 2005.

[7] Yi Andong, Zhang Dingguo. A Type of Light Hand Exoskeleton Based on Linear Motor. Mechanical Design and Research, 2019, 35(05):18-23.

[8] Moreno-Sanjuan V, Cisnal A, Fraile J C, et al. Design and characterization of a lightweight underactuated RACA hand exoskeleton for neurorehabilitation. Robotics and Autonomous Systems, 2021, 143:103828.

[9] Luo Mingzhou, Mei Tao, Lu Chaohong, Yu Yong. Analysis and simulation of enveloping grasp stability of the multi phalange underactuated robot hand. Optics and Precision Engineering, 2004.

[10] Zhao Jing. The Dynamic Analysis of a Controllable Underactuated Robot. Wuhan University of Technology, 2013.

[11] Sandoval-Gonzalez O, Jacinto-Villegas J, Herrera-Aguilar I, et al. Design and Development of a Hand Exoskeleton Robot for Active and Passive Rehabilitation. International Journal of Advanced Robotic Systems, 2016, 13(66): 1-12.